SUPPORTING INFORMATION

Comparative cranial myology and biomechanics of *Plateosaurus* and *Camarasaurus* and evolution of the sauropod feeding apparatus

by DAVID J. BUTTON[1,2,3], PAUL M. BARRETT[2] *and* EMILY J. RAYFIELD[1]

[1]School of Earth Sciences, University of Bristol, Life Sciences Building, 24 Tyndall Avenue, Bristol, BS8 1TQ; e-mail: e.rayfield@bristol.ac.uk

[2]Department of Earth Sciences, The Natural History Museum, London, SW7 5DB, UK; e-mail: p.barrett@nhm.ac.uk

[3]*Current address*: School of Geography, Earth and Environmental Sciences, University of Birmingham, Edgbaston, Birmingham, B15 2TT, UK; e-mail: d.j.button@bham.ac.uk

TABLE OF CONTENTS

VIRTUAL OSTEOLOGICAL RECONSTRUCTION

The skulls and right mandible of CMNH 11338, a juvenile *Camarasaurus lentus* (Figure S1) were CT scanned at the O'Bleness Memorial Hospital, Ohio, by L. M. Witmer. This yielded a stack of 326 slices of a slice thickness of 1 mm. These scans were then made available for use in this study by L. M. Witmer.

CT scan data of MB.R. 1937, the skull and both mandibles of an adult *Plateosaurus engelhardti* (figure S2) were also provided to the working group by L. M. Witmer, with the permission of R. Goessling on behalf of the Humbolt Museum für Naturkunde. The specimen was originally scanned at the Humboldt Museum für Naturkunde at the Faculty of Veterinary Medicine, Freie Universität, Berlin by R. Goessling as part of an unconnected study. This yielded a stack of 281 slices for the skull and 273 for each mandible with a slice thickness of 1.25 mm.

These scan data were imported into Avizo (versions 6.3.1, 7 and 8.0 FEI Visualization Science Group) for segmentation. Each specimen has suffered taphonomic deformation, with missing and warped elements; this was reversed utilising transformation, translation and mirroring tools within Avizo in order to produce a reconstruction of the cranial osteology as it would have been in-life for each taxon. Retrodeformaton followed a protocol of using better-preserved elements to help constrain the positions of those which are more poorly known; this is described for each taxon below. The skull reconstruction performed for *Camarasaurus* was previously used in the analyses of Button *et al*. (2014) and that of *Plateosaurus* in the analyses of Lautenschlager *et al*. (2016), but the retrodeformation process for each is described in more detail below.

Camarasaurus – the skull and mandible of CMNH 11338 are in general very well preserved (Figure S1). However the exposed left premaxilla, maxilla, nasal, lacrimal postorbital, jugal, squamosal, quadraojugal, quadrate and palate have suffered some medial displacement, the left

prefrontal has suffered multiple fractures, and the left mandible has been separated from the specimen. In contrast, the right hand side of the skull remains largely buried in matrix and these elements mostly retain their original geometry. These were hence mirrored and used to replace their deformed counterparts from the left side of the skull. The right premaxilla remains slightly deformed and required twisting of the ascending process and anteromedial margin to restore the original flat surface it presented at the midline. Additionally, the skull roof bears multiple cracks which were infilled, and the surrounding bones pushed back together where necessary. The completed osteological model is given in Figure S3.

Plateosaurus – MB.R. 1937 has suffered greater deformation, with the skull having been laterally compressed and dorsoventrally sheared (Figure S2). After segmentation the skull was virtually disarticulated, and the best preserved example of each paired element was selected to form the basis of further reconstruction. In most cases this was the example from the left side of the skull; the right side has suffered more extensive dorsal and medial displacement (Figure S2). However, the descending processes of the nasal and postorbital, ascending process of the jugal and paraoccipital process from the right side of the skull were all considered to be better preserved than their antimeres. These were mirrored and combined with the appropriate elements from the left side of the skull to produce composite reconstructions of each. Other obvious damage such as cracks, holes and warpage to these selected elements was then repaired, with comparison to other *Plateosaurus* specimens (Galton 1984, 1985), particularly the well-preserved and complete *Plateosaurus erlenbergiensis* skull and mandible AMNH FARB 6810 (Galton 1984; Prieto-Márquez & Norell 2011).

Further repair and rearticulation were then performed concurrently and in systematic order, with the best preserved elements treated first. Again, comparison was made throughout to the proportions of other *Plateosaurus* specimens and previous cranial reconstructions (Galton 1984, 1985; Yates 2003; Galton & Upchurch 2004; Prieto-Márquez & Norell 2011) to ensure

consistency. The left parietal, frontal, squamosal, quadrate and braincase were deemed to be the least deformed elements and so these were restored first. These elements were then mirrored across the bilaterally symmetrical long axis of the skull to produce their antimeres. The repaired left maxilla was also then rearticulated with its mirrored antimere along the midline. These reconstructed snout and skull roof regions then provided greater constraint on the morphology of more poorly preserved elements, which were then reconstructed in turn. The premaxillae were next rearticulated with the maxillae, after repair of the warped premaxillar ascending process to provide a flat medial articular surface with the opposing premaxilla. The restored maxilla and premaxilla then allowed rearticulation of the nasals. Compression had led to lateromedial buckling of the nasals; this was corrected after rearticulation. The jugals were next rearticulated with the maxillae; these, the frontals and the quadrate then helped to constrain the morphology of the postorbital and quadratojugal which were repaired and rearticulated. The repaired lacrimal was then rearticulated with the maxilla, nasals and frontal, and the prefrontal with the frontal and lacrimal. The ectopterygoids, vomers and palatines were then rearticulated with the facial bones and used to help constrain the reconstruction of the pterygoids, which have been heavily crushed in MB.R. 1937. The epipterygoids of MB.R. 1937 have also suffered considerable damage; these were reconstructed after those of AMNH FARB 6810 and rearticulated with the quadrate and braincase (Prieto-Márquez & Norell 2011). Finally, the orbitosphenoids of MB.R. 1937 are entirely absent. These were hence manually reconstructed from those of other sauropodomorphs and rearticulated with the braincase.

The mandibles of MB.R. 1937 are less deformed than the skull, but have suffered lateromedial flattening and extensive surface cracking. This damage was then repaired in the left mandible, with the curvature of the upper toothrow used as a guide in restoration of the original curve of the dentary. The completed left mandible was then mirrored, and the two mandibles rearticulated at the symphysis. The completed osteological model is given in Figure S4.

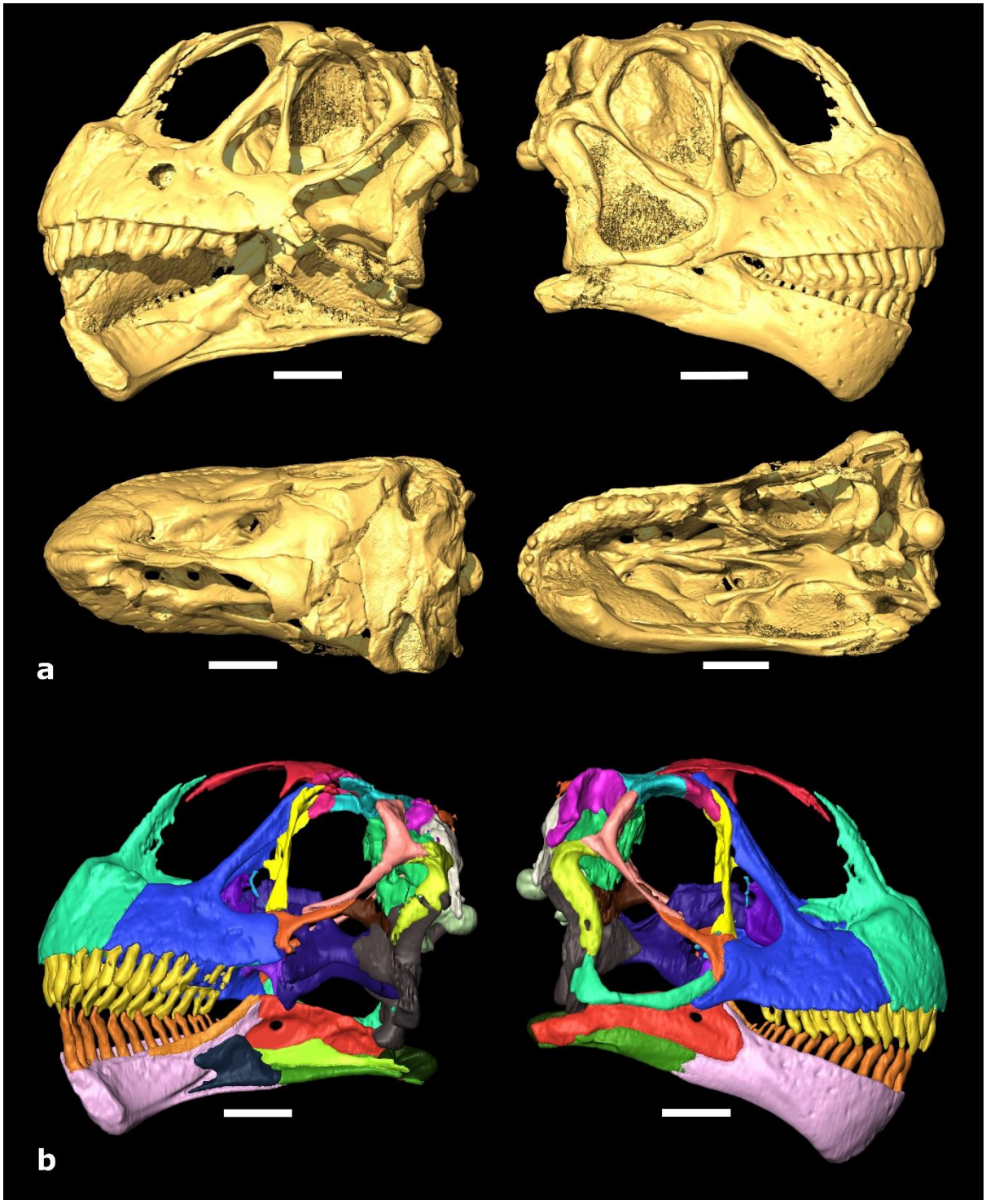

Figure S1: *Camarasaurus lentus* CMNH 11338. a) Isosurface of the skull in (clockwise from left) left lateral, right lateral, ventral and dorsal views. b) Surface model produced from segmentation of CT scans. Left: skull in left lateral view and right mandible in medial view. Right: Skull and right mandible in right lateral view. Scale bars = 50 mm.

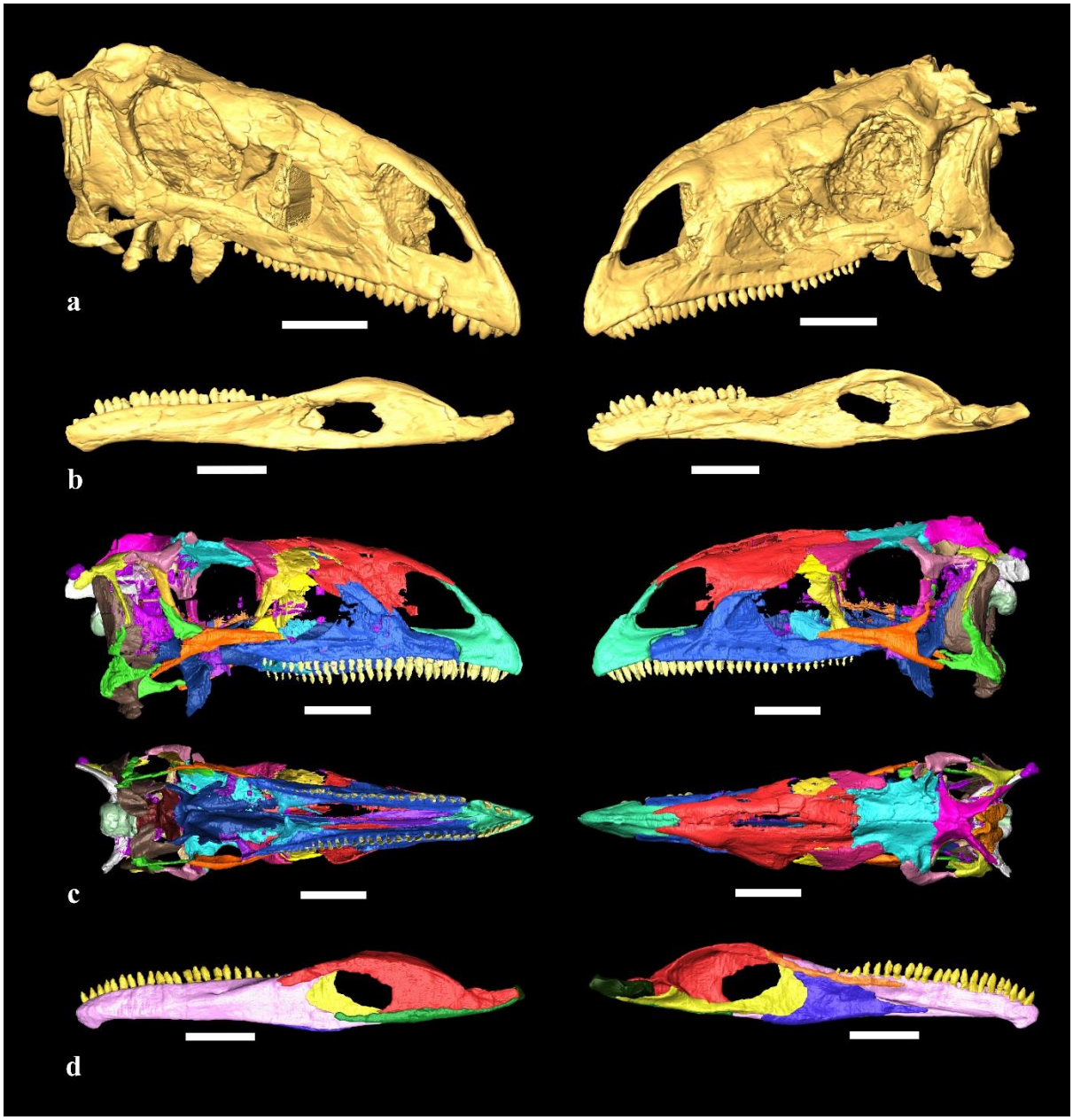

Figure S2: *Plateosaurus engelhardti* MB.R. 1937. a) Isosurface of the skull in right oblique (left) and left oblique (right) views. b) Isosurfaces of the mandibles; left: left mandible in lateral view, right: right mandible in medial view. c) Surface model of MB.R. 1937 produced from segmentation of CT scans in right lateral (top left), left lateral (top right) ventral (bottom left) and dorsal (bottom right) views. d) Segmented mandibles; left: left mandible in lateral view, right: left mandible in medial view. Scale bars = 50 mm.

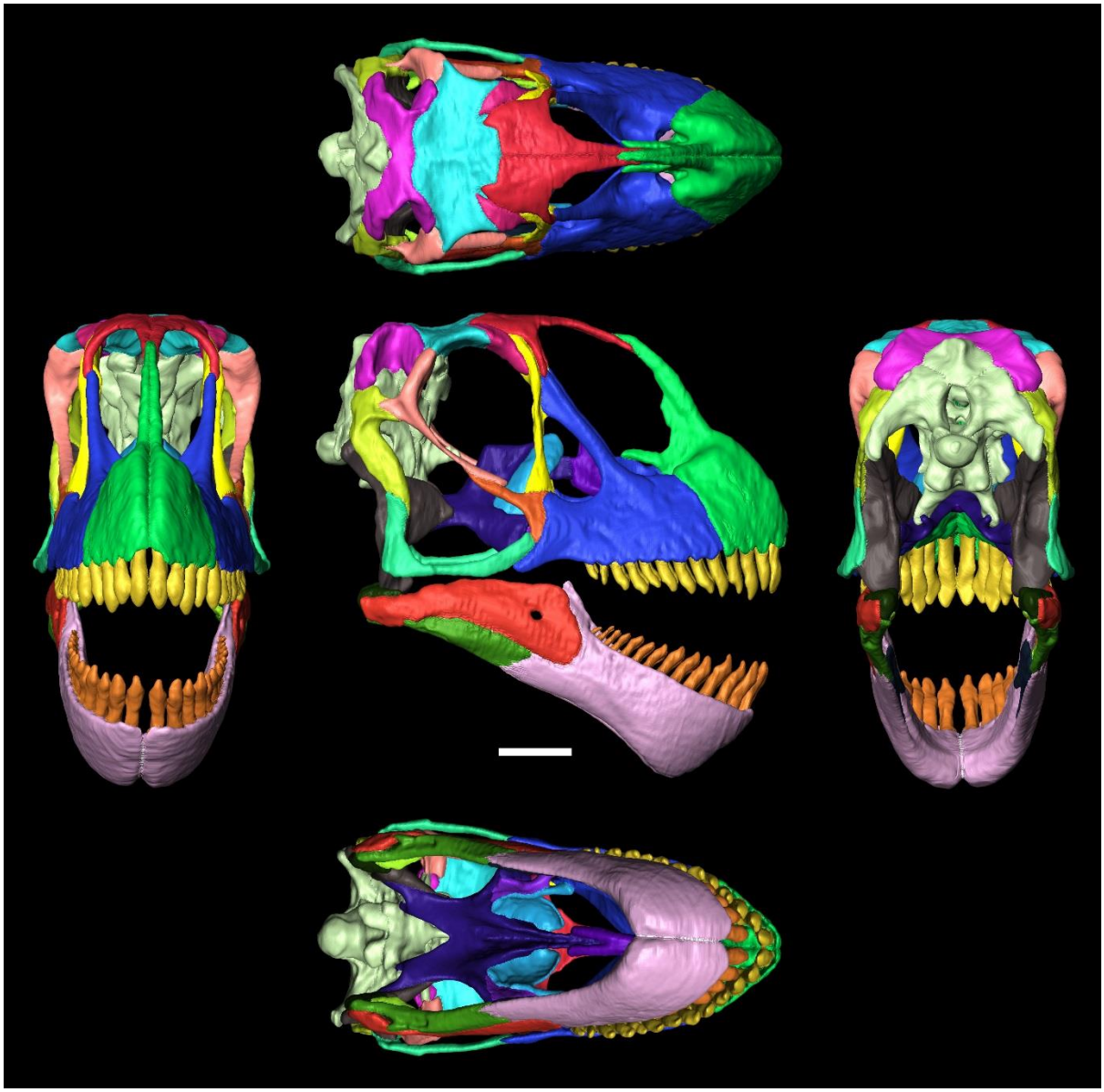

Figure S3: Cranial osteological reconstruction of *Camarasaurus lentus*. Shown in right lateral view (centre) and (clockwise from left) anterior, dorsal, posterior and ventral views. Scale bar = 50 mm.

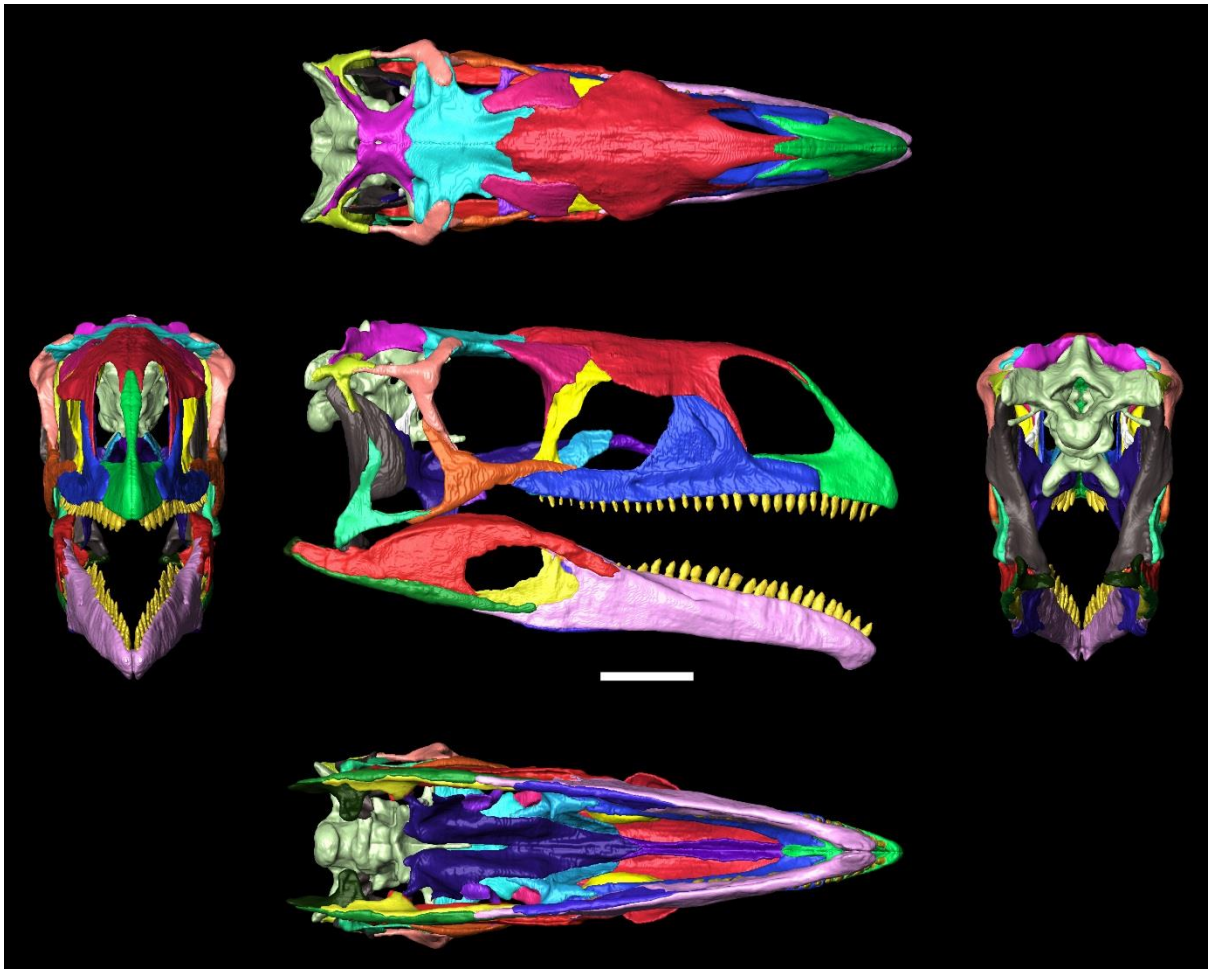

Figure S4: Cranial osteological reconstruction of *Plateosaurus engelhardti*. Shown in right lateral view (centre) and (clockwise from left) anterior, dorsal, posterior and ventral views. Scale bar = 50 mm.

MYOLOGICAL RECONSTRUCTION ADDITIONAL RESULTS

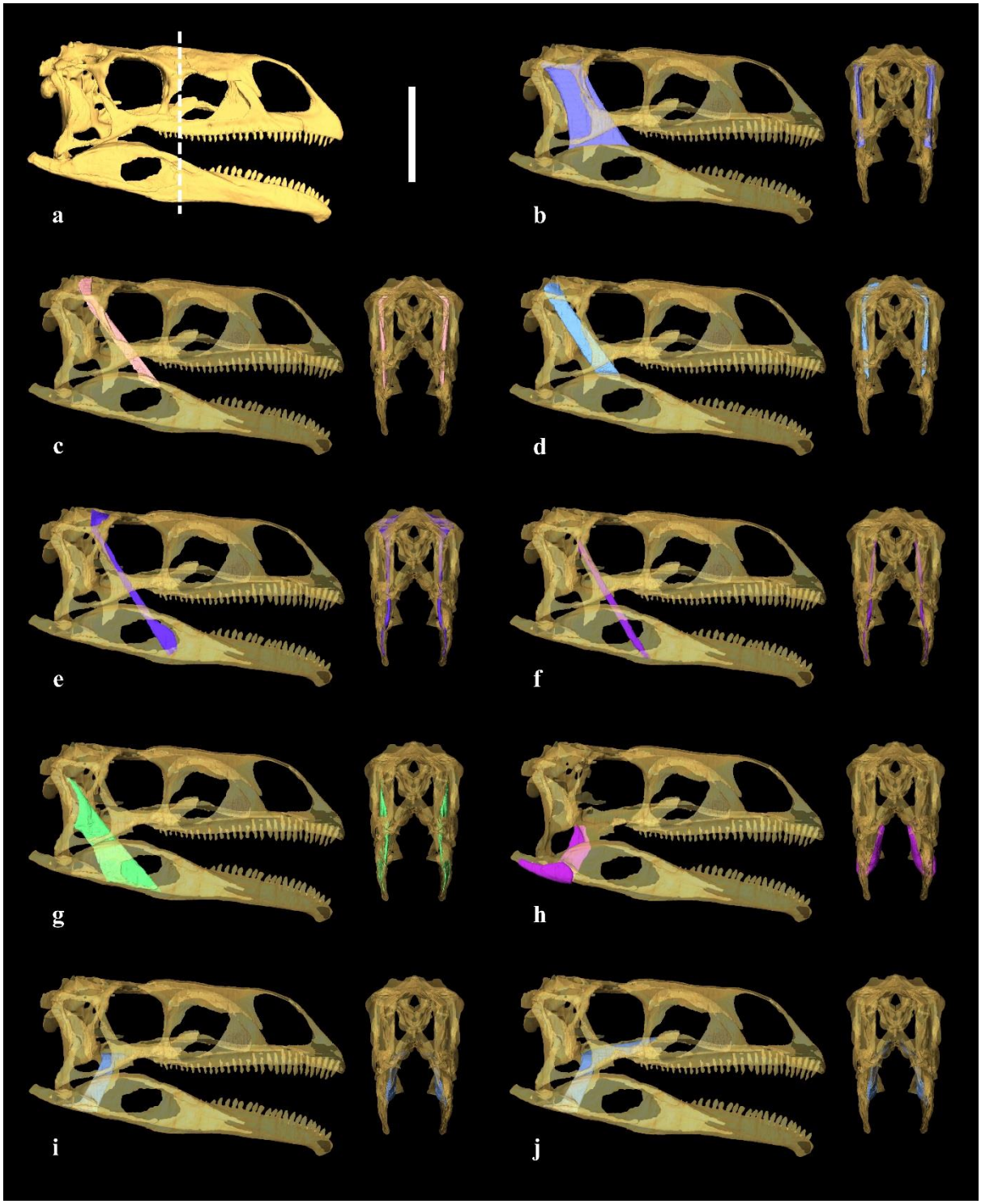

Figure S5: a) Skull of *Plateosaurus* right lateral view. Dotted line indicates the position of coronal section used in b-j). b-J) Individual muscle reconstructions, with the skull rendered semi-transparent. Each shown in lateral view (left) and anterior view of a coronal section taken along the dotted line shown in a) (right). Muscles shown as follows: b) m.AMES, c) m.AMEP, d) m.AMEM, e) m.PSTs, f) m.PSTp, g) m.AMP, h) m.PTv, i) m.PTd, j) alternate, more expansive, reconstruction of the m.PTd.

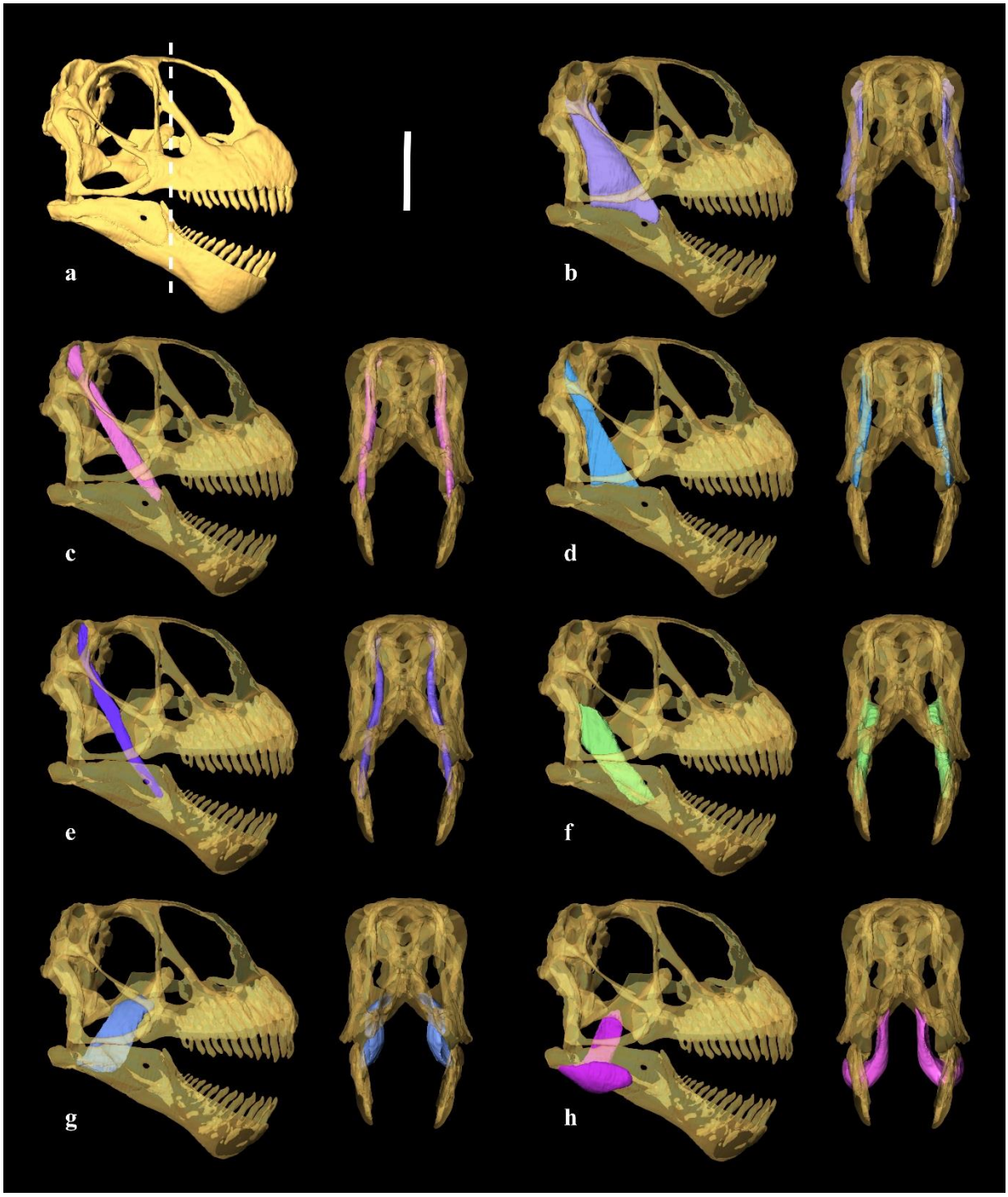

Figure S6: a) Skull of *Camarasaurus* in right lateral view, dotted line indicates the position of the coronal section taken in b-i). Individual muscle reconstructions, with the skull rendered semi-transparent. Each shown in lateral view (left) and anterior view of a coronal section taken along the dotted line shown in a) (right). Muscles shown as follows: b) m.AMES, c) m.AMEP, d) m.AMEM, e) m.PSTs, f) m.PSTp, g) m.AMP, h) m.PTd, i) m.PTv.

FINITE ELEMENT ANALYSIS ADDITIONAL RESULTS

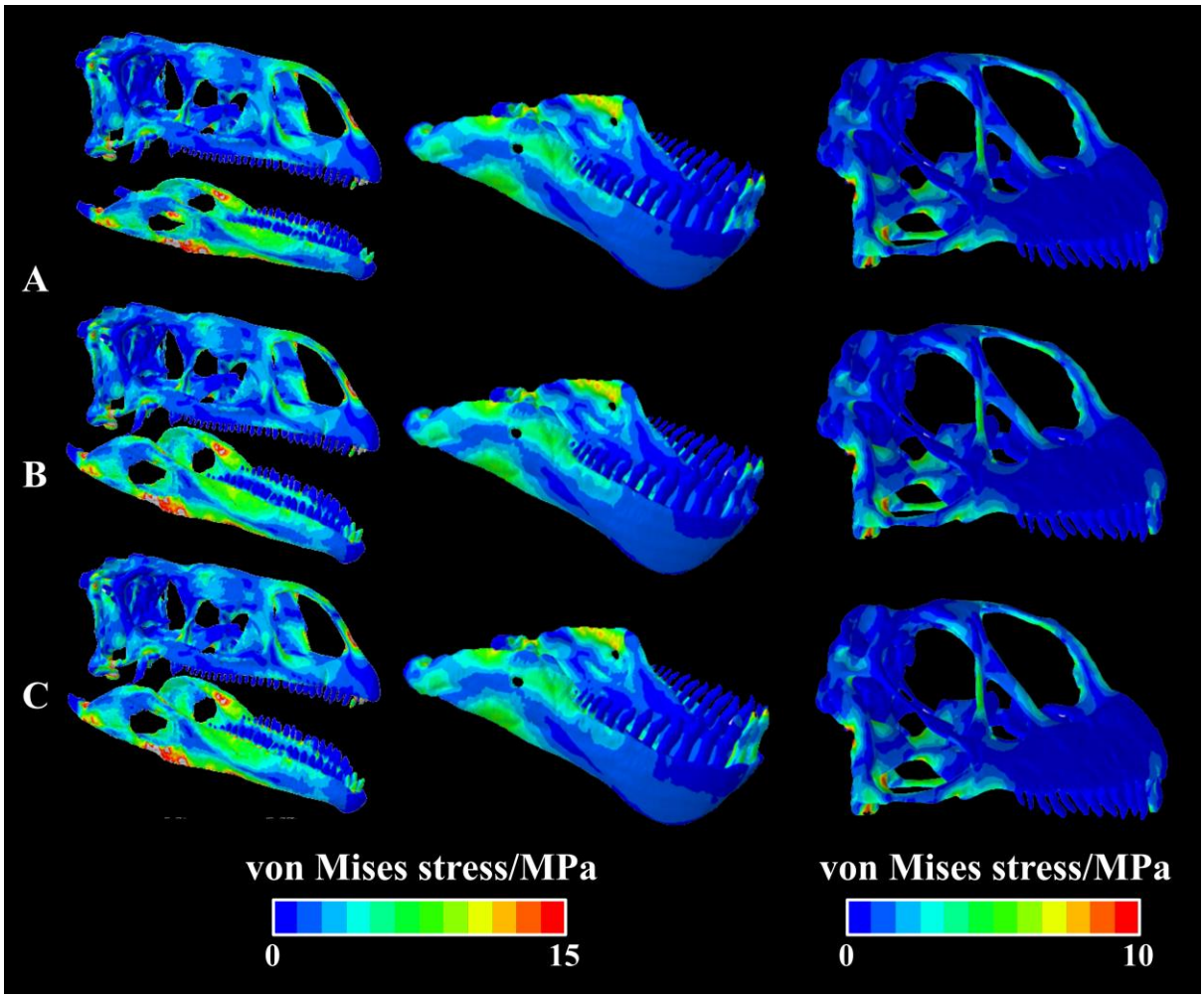

Figure S7: von Mises contour plots of the skull of *Plateosaurus* (left) and mandible (middle) and cranium (right) of *Camarasaurus*, showing the influence of altering the material properties of the teeth. A) Results with the teeth modelled as a single, composite material; B) results with the teeth ascribed the material properties of vertebrate enamel; C) results with the teeth ascribed the material properties of dentine. The influence of the way in which the teeth were treated on results can be seen to have very little impact on overall stress patterns and magnitudes. Note the change in scale between the *Plateosaurus* and *Camarasaurus* mandible results from those for the *Camarasaurus* cranium.

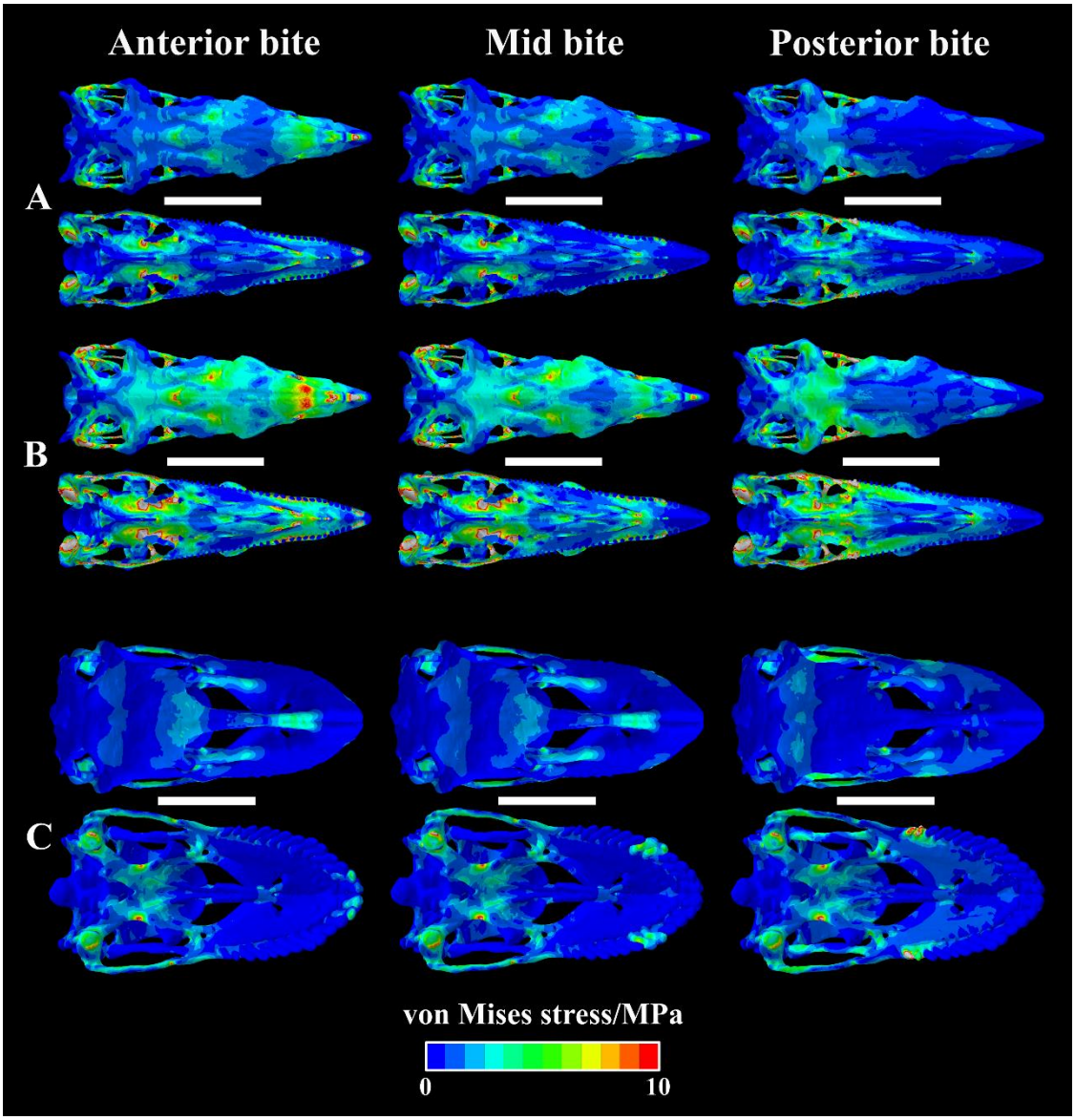

Figure S8: von Mises stress contour plots from FEA of the crania of *Plateosaurus* and *Camarasaurus* for anterior (left), mid (middle) and posterior (right) bilateral biting positions, in dorsal (top) and ventral (bottom) views. A) Results for the unscaled *Plateosaurus* model. B) Results for "structural comparison" model of *Plateosaurus*, scaled so that total applied muscle force:skull surface area is equal to that of *Camarasaurus*. C) Results for *Camarasaurus*. Scale bars = 100 mm.

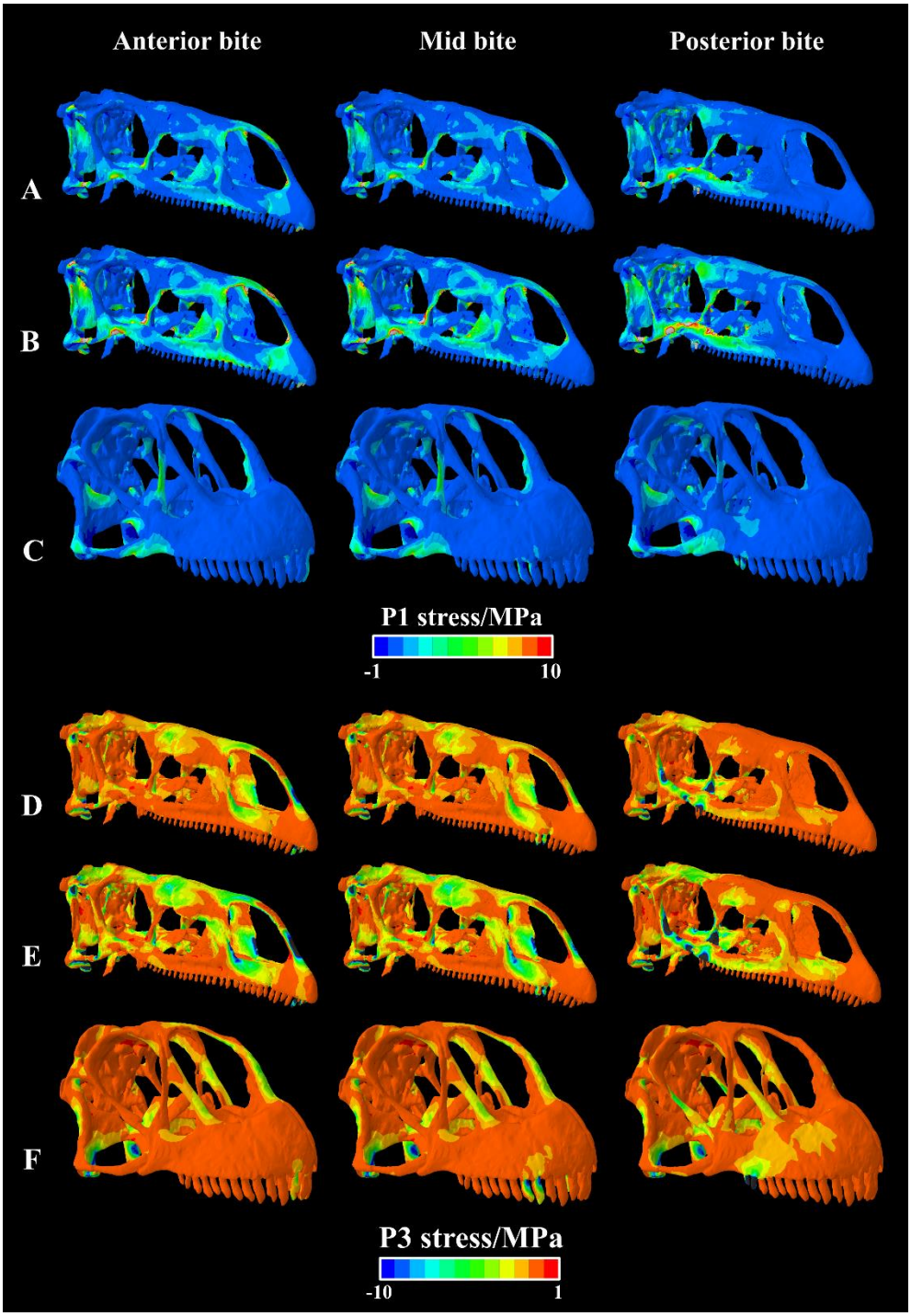

Figure S9: Principal stress contour plots from FEA of the crania of *Plateosaurus* and *Camarasaurus* for the three bilateral biting positions, in oblique lateral view. A-C) P1 (principally tensile) stress plots; more positive values refer to greater tensile stress. A) Unscaled *Plateosaurus* model. B) Scaled ('structural comparison') *Plateosaurus* model. C) *Camarasaurus* model. D-F) P3 (principally compressive) stress plots; more negative values refer to greater compressive stress. D) Unscaled *Plateosaurus* model. E) Scaled ('structural comparison') *Plateosaurus* model. F) *Camarasaurus* model.

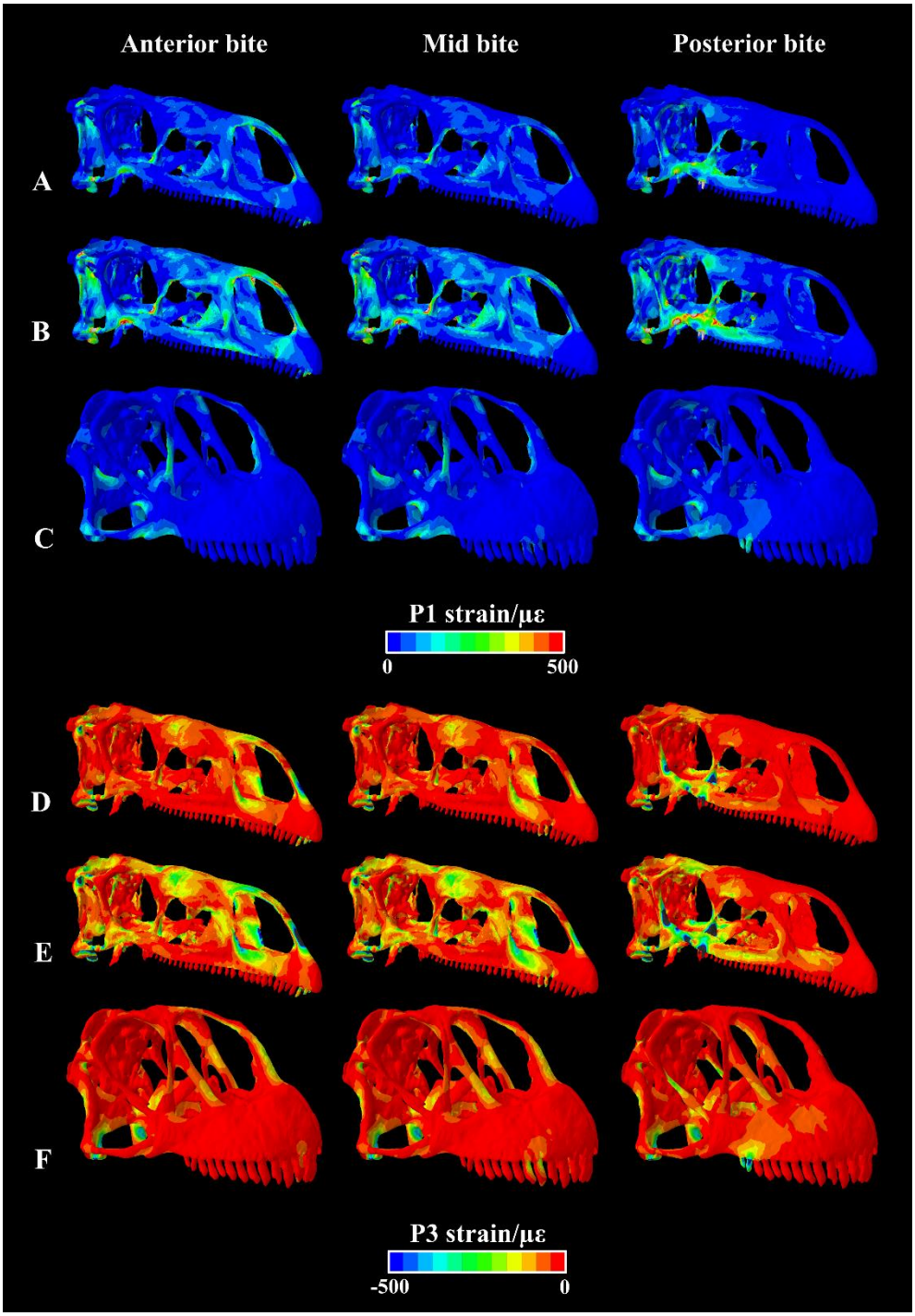

Figure S10: Principal strain contour plots from FEA of the crania of *Plateosaurus* and *Camarasaurus* for the three bilateral biting positions, in oblique lateral view. A-C) P1 (principally tensile) strain plots; more positive values refer to greater tensile stress. A) Unscaled *Plateosaurus* model. B) Scaled ('structural comparison') *Plateosaurus* model. C) *Camarasaurus* model. D-F) P3 (principally compressive) strain plots; more negative values refer to greater compressive stress. D) Unscaled *Plateosaurus* model. E) Scaled ('structural comparison') *Plateosaurus* model. F) *Camarasaurus* model.

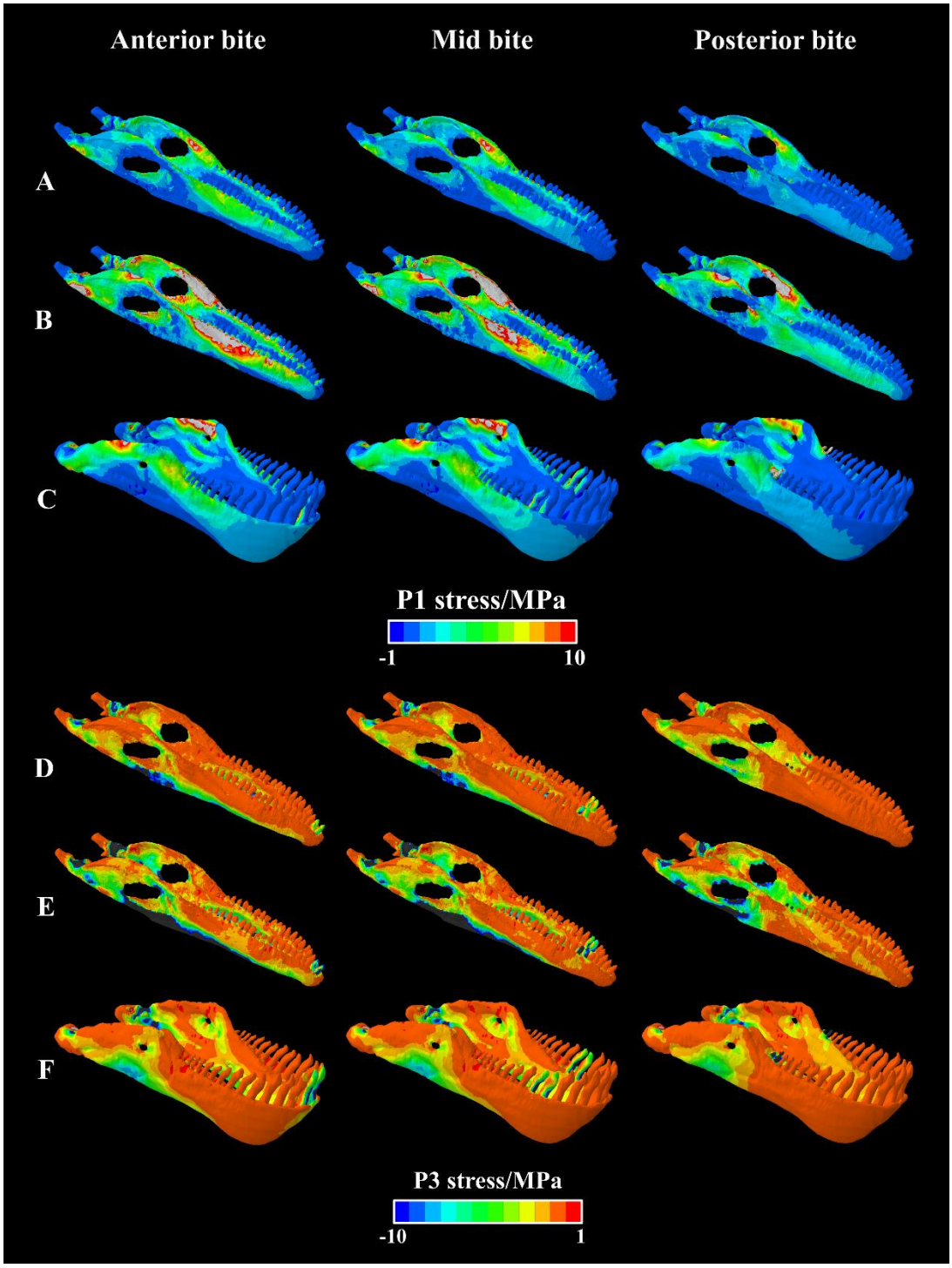

Figure S11: Principal stress contour plots from FEA of the mandibles of *Plateosaurus* and *Camarasaurus* for the three bilateral biting positions, in oblique lateral view. A-C) P1 (principally tensile) stress plots; more positive values refer to greater tensile stress. A) Unscaled *Plateosaurus* model. B) Scaled ('structural comparison') *Plateosaurus* model. C) *Camarasaurus* model. D-F) P3 (principally compressive) stress plots; more negative values refer to greater compressive stress. D) Unscaled *Plateosaurus* model. E) Scaled ('structural comparison') *Plateosaurus* model. F) *Camarasaurus* model.

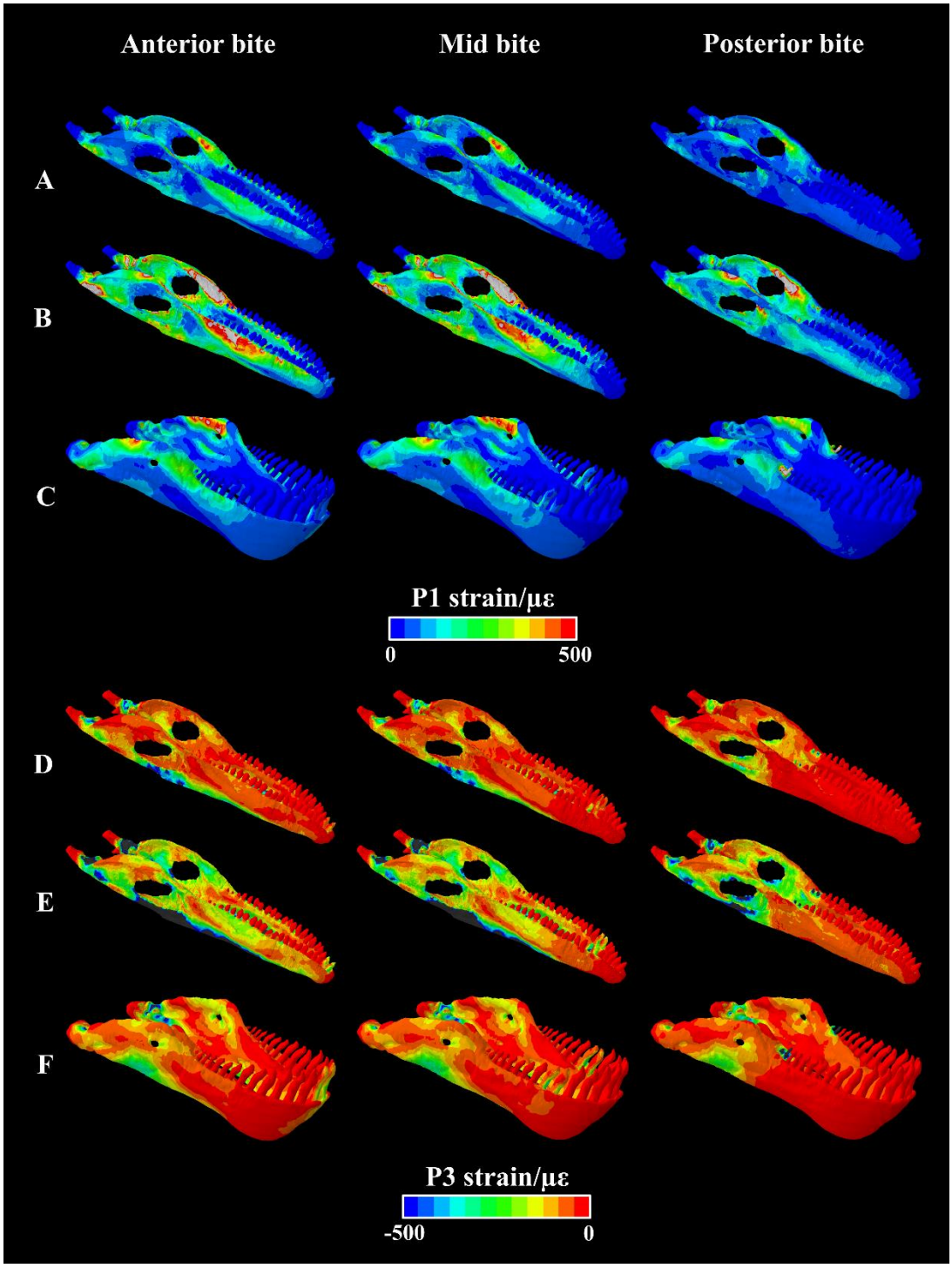

158

159 Figure S12: Principal strain contour plots from FEA of the mandibles of *Plateosaurus* and *Camarasaurus* for the
160 three bilateral biting positions, in oblique lateral view. A-C) P1 (principally tensile) strain plots; more positive
161 values refer to greater tensile stress. A) Unscaled *Plateosaurus* model. B) Scaled ('structural comparison')
162 *Plateosaurus* model. C) *Camarasaurus* model. D-F) P3 (principally compressive) strain plots; more negative
163 values refer to greater compressive stress. D) Unscaled *Plateosaurus* model. E) Scaled ('structural comparison')
164 *Plateosaurus* model. F) *Camarasaurus* model.

SUPPLEMENTARY REFERENCES

GALTON, P. M. 1984. Cranial anatomy of the prosauropod dinosaur *Plateosaurus* from the Knollenmergel (Middle Keuper, Upper Triassic) of Germany. I. Two complete skulls from Trossingen/Württ. With comments on the diet. *Geologica et Palaeontologica*, **18**, 139–171.

——— 1985. Cranial anatomy of the prosauropod dinosaur *Plateosaurus* from the Knollenmergel (Middle Keuper, Upper Triassic) of Germany. II. All the cranial material and details of soft-part anatomy. *Geologica et Palaeontologica*, **19**, 119-159.

——— and UPCHURCH, P. 2004. Prosauropoda. *In:* WEISHAMPEL, D. B., DODSON, P. and OSMÓLSKA, H. (eds). *The Dinosauria (2nd Edn.)*. University of California Press, Berkerly, USA, 232-258.

LAUTENSCHLAGER, S., BRASSEY, C., BUTTON, D. J. & BARRETT, P. M. 2016. Decoupled form and function in disparate herbivorous dinosaur clades. *Scientific Reports*, **6**, 26495.

MADSEN, J. H. Jr., MCINTOSH, J. S. and BERMAN, D. S. 1995. Skull and atlas-axis complex of the Upper Jurassic sauropod *Camarasaurus* (Reptilia: Saurischia). *Bulletin of Carnegie Museum of Natural History*, **31**, 1-115.

PRIETO-MÁRQUEZ, A. and NORELL, M. A. 2011. Redescription of a nearly complete skull of *Plateosaurus* (Dinosauria: Sauropodomorpha) from the Late Triassic of Trossingen (Germany). *American Museum Novitates*, **3727**, 1-58.

YATES, A. M. 2003. The species of taxonomy of the sauropodomorph dinosaurs from the Löwenstein Formation (Norian, Late Triassic) of Germany. *Palaeontology*, **46**, 317-337.